JOURNAL OF THEORETICAL
AND APPLIED MECHANICS
3, **37**, 1999

A CONTRIBUTION TO EVALUATION OF EFFECTIVE MODULI OF TRABECULAR BONE WITH ROD-LIKE MICROSTRUCTURE

STANISŁAW TOKARZEWSKI

JÓZEF JOACHIM TELEGA

ANDRZEJ GAŁKA

Institute of Fundamental Technological Research Polish Academy of Sciences
e-mail:jtelega@ippt.gov.pl

The homogenization theory has been applied to evaluation of effective moduli of a network of interconnected elastic rods modelling human cancellous bone. Numerical computations of the Young modulus, Poisson ratio and shear modulus have been carried out. The obtained results compare fevourably with available experimental data.

Key words: trabecular bone, effective elastic moduli, homogenization

1. Introduction

Biological materials; like, animal and human bones are porous materials with complicated hierarchical structure. Bones occur in the two forms: as a dense solid (*compact bone*) and as a porous network of connected rods and plates (*cancellous or trabecular bone*). The most obvious difference between these two types of bones consists in their relative densities measured by a volume fraction of solids (see Fig.1, and Gibson and Ashby, 1988).

Both types can be found most bones in the body, the dense compact bone forming an outer shell surrounding a core of spongy cancellous bone. Idealizations of compact bone structures can be is seen in Fig.2 $\div$ Fig.4, in Telega et al. (1999), cf also Cowin (1989a).

Typical examples of trabecular bones with a rod-like microstructure are shown in Fig.2 and Fig.3. These figures provide interesting visualization of human trabecular bone architecture obtained by using the micro-computed

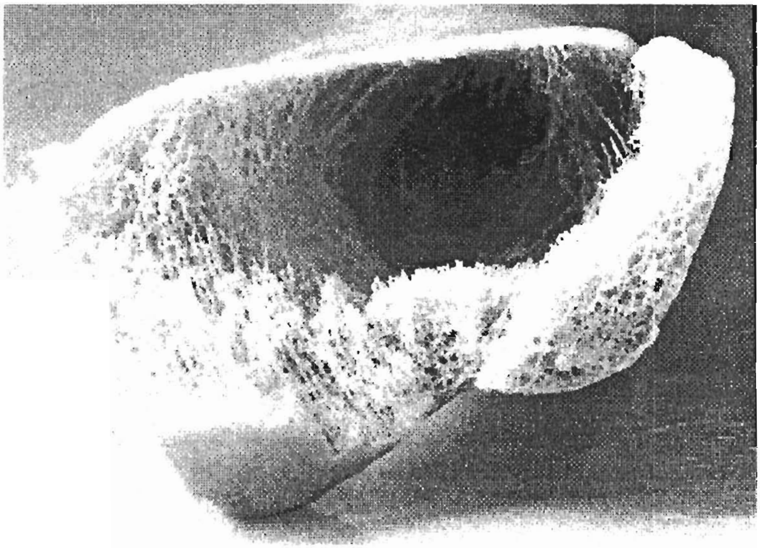

Fig. 1. Photograph of a proximal part of the human femur

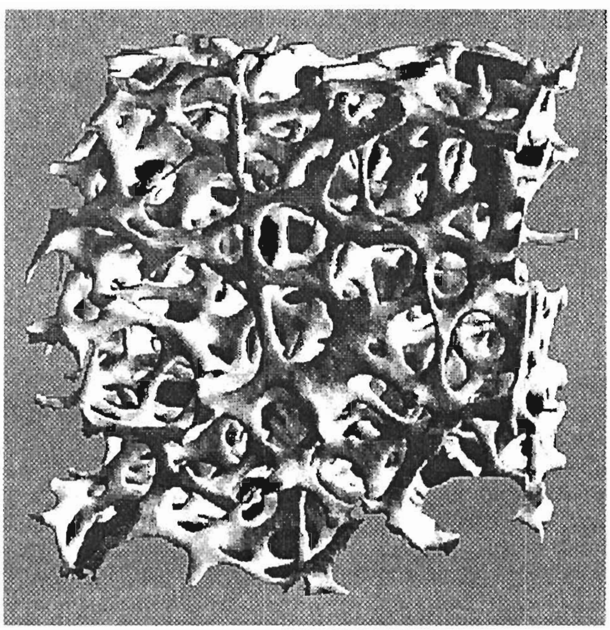

Fig. 2. Three-dimensional trabecular bone architecture of a lumber spine bone biopsy of a 42-year-old male. The distinct rod-like columnar structure can be easily seen, after Müller and Rüegsegger (1997)

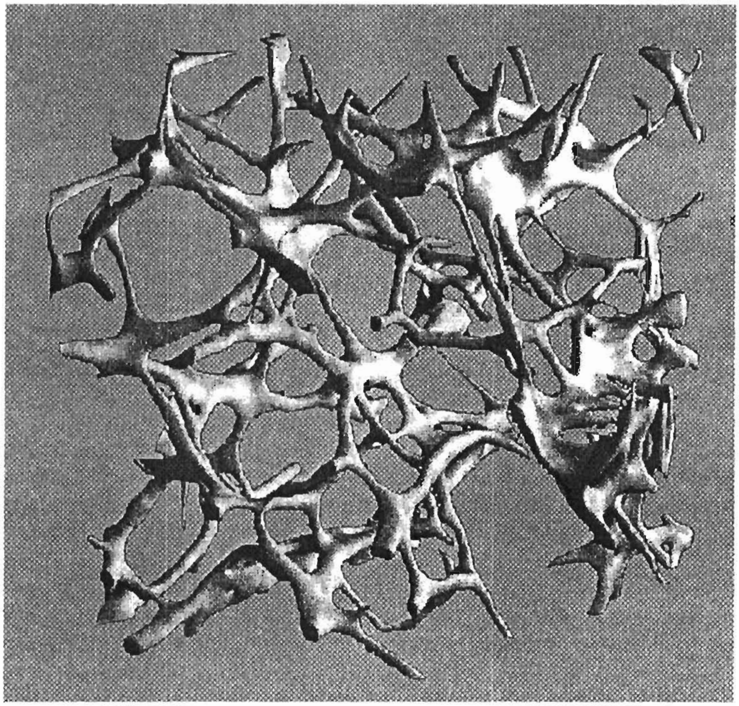

Fig. 3. Three-dimensional bone

tomography (Müller and Rüegsegger, 1997; Ulrich et al., 1997). According to Müller and Rüegsegger (1997) specimens with diameters of a few millimeters, up to 18 mm, can be measured. Such a bone is weaker than the bone with a plate-like microstructure examined in our previous paper (Gałka et al., 1999). Typical models of the structure of a cancellous bone are sketched in Fig.4.

In Fig.2 and Fig.3 the size of the VOI (selected volume of interest amounts to $4\times4\times4\,\mathrm{mm}^3$ ($286\times286\times286$ voxels). For related studies on bone structure the reader is referred to Lowet et al. (1997).

Microstructure analyses of trabecular bone have followed the general approach used in modelling the cellular plastics. McElhaney et al. (1970) developed a porous block model of trabecular bone based on composing of spring stiffness loaded in parallel or in series. Using this model, they found a good agreement between theprediction of apparent stiffness and the experimentally results in some internal layer of the human skull. Pugh et al. (1973) modelled the subchondral trabecular bone as a collection of structural plates and concluded that bending and buckling were major modes of deformation of the trabecular. Williams and Lewis (1982) modelled the exact structure of a 2D

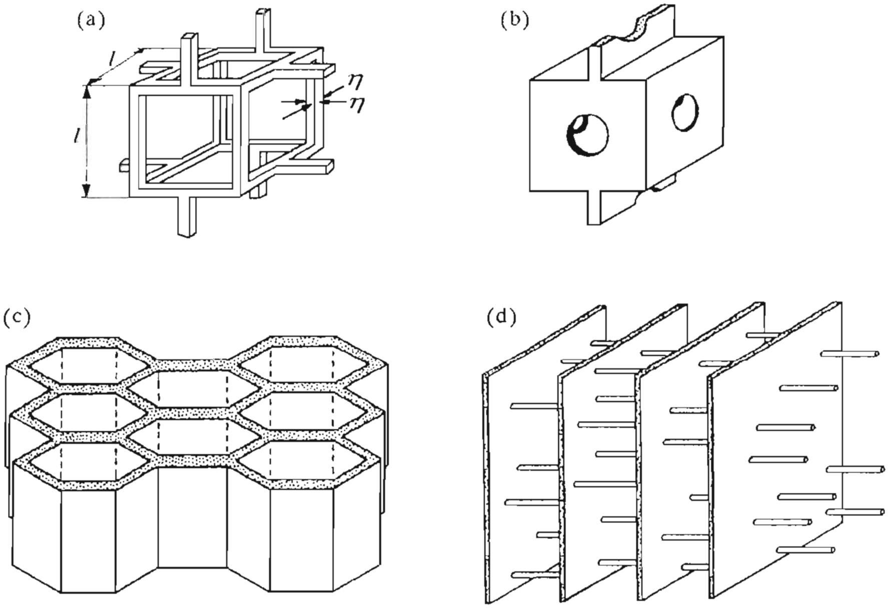

Fig. 4. Models of the structure of cancellous bone: (a) low density equiaxed structure, (b) higher-density equiaxed structure, (c) stress oriented prismatic structure, (d) stress-oriented parallel plate structure, after Gibson and Ashby (1988)

section of trabecular bone using the plane strain finite elements to predict the apparent transversely isotropic elastic constants. Gibson (1985) developed models of trabecular bone structure using analytical techniques for porous solids. He predicted dependence of the apparent stiffness on the apparent density for different structural types of trabecular bones. Beaupré and Hayes (1985) developed a 3D spherical void model of trabecular bone and used finite element analysis to predict the apparent stiffness and strength, as well as the stress distribution within the trabecular bone. Hollister et al. (1991, 1994) applied the homogenization theory (Bensoussan et al., 1978; Lewiński and Telega, 1999; Sanchez-Palencia, 1980) to investigation of mechanical behaviour of the cubic rods-like structures modelling trabecular bones. By using finite element method they evaluated apparent orthogonal Young moduli and compared them with the experimental results obtained for proximal humerus, proximal tibia and distal femur. To take into account the influence of bone marrow, Kasra and Grynpas (1998) performed suitable numerical calculation. Bone may be viewed as a structurally hierarchical porous material. It is then possible to use the reiterated homogenization to derive the formulae for the macroscopic elastic moduli, cf Telega et al. (1999). Optimal design of structures often involves homogenization and relaxation methods (Bendsøe, 1995; Bendsøe and Kikuchi, 1988; Kohn and Strang, 1986; Lewiński and Telega, 1999; Lurie et al., 1982). Such an approach may be used to model the bone microstructure via adaptive elasticity. Payten et al. (1998) presented an optimisation process based on an algorithm originally developed for predicting anatomical density distributions in natural human bone.

The microstructure of bone is such that at the macroscopic level its behaviour is anisotropic. To model bone anisotropy one can use Cowin's fabric tensor, see Cowin (1989b), Jemioło and Telega (1998); Lowet et al. (1997) and the references cited therein. Jemioło and Telega (1998) demonstrated that a compact bone reveals properties close to transverse isotropy whilst a trabecular bone is approximately orthotropic, cf also Zysset et al. (1998). The approach employed in Jemioło and Telega (1998) exploits Cowin's fabric tensor. In Zysset et al. (1998) the authors claim to use a homogenization method for finding the orthotropic elastic constants, yet, unfortunately, no precise formulation was given.

Warren and Kraynik (1997) analysed the linear elastic behaviour of an open-cell like Kelvin foam by relating forces and distorsion at the strut level to a macroscopic response. Such a cellular solid seems to be inappriopriate for a trabecular bone.

The goal of the present contribution is to estimate the elastic macroscpic properties of cancellous bone with a rod-like architecture. An idea sketched by Tokarzewski et al. (1998) is developed in Sections 3 and 4. The method developed by Gałka et al. (1999) does not apply to the case presened in Fig.7, which is of interest here. The basic cell problem is therefore solved approximately, by using a typical structural mechanics approach. Primarily, however, in Section 2 basic formulae for the homogenization of porous linear elastic solids are summarized. The reiterated homogenization was used in our paper (Telega et al. 1999) for derivation of the macroscopic elastic properties of a compact bone. The available results of calculation were also briefly reviewed.

2. Homogenization of porous elastic materials

Let Ω denote a bounded open subset of $\mathbb{R}^3$. As usual by Y we denote the basic cell, cf Bensoussan at al. (1978), Dal Maso (1993), Jikov et al. (1994), Lewiński and Telega (1999), Sanchez Palencia (1980). The part of Y occupied by the material is denoted by Y_t. The considerations which follow are formal from the mathematical point of view. By Ω_t^ε we denote the part of Ω occupied by the material. Here $\varepsilon > 0$ is a small parameter.

Let us consider the following boundary value problem of linear elasticity:

$$\begin{aligned} &\frac{\partial}{\partial x_j}\Big[a_{ijkl}\Big(\frac{\boldsymbol{x}}{\varepsilon}\Big)\frac{\partial u_k^\varepsilon}{\partial x_l}\Big] + f_i = 0 && \text{in} \quad \Omega_t^\varepsilon \\ &u_k^\varepsilon = 0 && \text{on} \quad \partial\Omega \\ &a_{ijkl}\Big(\frac{\boldsymbol{x}}{\varepsilon}\Big)\frac{\partial u_k^\varepsilon}{\partial x_l}n_j = 0 && \text{on} \quad \partial\Omega_t^\varepsilon\backslash\partial\Omega \end{aligned} \tag{2.1}$$

where $\boldsymbol{n} = (n_j)$ is the unit vector normal to $\partial\Omega_t^\varepsilon\backslash\partial\Omega$ and $\boldsymbol{u}^\varepsilon$ stands for the displacement vector.

We make the following assumptions:

(i) $f \in L^2(\Omega)$,

(ii) $a_{ijkl} \in L^\infty(Y_t)$, $i,j,k,l = 1,2,3$.

(iii) There exists a positive c_0 such that for almost every $y \in Y_t$ constant

$$a_{ijkl}(\boldsymbol{y})e_{ij}e_{kl} \geqslant C_0 e_{ij}e_{ij} \quad \text{for any } \boldsymbol{e} = (e_{ij}) \quad e_{ij} = e_{ji}$$

(iv) The material coefficients $a_{ijkl}(\boldsymbol{y})$ are Y-periodic.

The displacement field $\boldsymbol{u}^h$ of the homogenized solid is a solution to

$$\begin{aligned} &q_{ijkl}\frac{\partial^2 u_k^h}{\partial x_j \partial x_l} + \frac{|Y_t|}{|Y|}f_i = 0 && \text{in} \quad \Omega \\ &\boldsymbol{u}^h = \boldsymbol{0} && \text{on} \quad \partial\Omega \end{aligned} \tag{2.2}$$

Here $|Y| = \mathrm{vol}Y$, $|Y_t| = \mathrm{vol}Y_t$. The homogenized coefficients q_{ijkl} are given by

$$q_{ijmn} = \langle a_{ijmn}\rangle - \Big\langle a_{ijpq}\frac{\partial \chi_p^{(mn)}}{\partial y_q}\Big\rangle \tag{2.3}$$

where

$$\langle\cdot\rangle = \frac{1}{|Y|}\int\limits_{Y_t}(\cdot)\,d\boldsymbol{y}$$

The Y-periodic functions $\chi_p^{(mn)}$ are solutions to the local problem

$$\begin{aligned} &\frac{\partial}{\partial y_i}\Big[a_{ijmn}\frac{\partial}{\partial y_n}(\chi_m^{(pq)} - \delta_{mp}y^q)\Big] = 0 && \text{in} \quad Y_t \\ &\frac{\partial}{\partial y_n}\Big[a_{ijmn}(\chi_m^{(pq)} - \delta_{mp}y^q)\Big]N_i = 0 && \text{on holes boundaries} \end{aligned} \tag{2.4}$$

Written in the weak form, this problem is expressed by

$$\int_{Y_t} a_{ijmn} \frac{\partial \chi_m^{(pq)}}{\partial y_n} \frac{\partial \Psi_j}{\partial y_i} \, d\boldsymbol{y} = - \int_{Y_t} a_{ijpq} \frac{\partial \Psi_j}{\partial y_i} \, d\boldsymbol{y} \quad \forall \, \Psi_j \in H_{per}(Y_t) \tag{2.5}$$

where

$$H_{per}(Y_t) = \Big\{ v \in H^1(Y_t) : \; v \text{ is } Y - \text{periodic} \Big\}$$

By putting $\chi_i^{rs}(\boldsymbol{y}) = \delta_{ir}\boldsymbol{y} - U_i^{rs}(\boldsymbol{y})$ we rewrite Eq (2.3) in the following form

$$q_{ijrs} = \Big\langle a_{ijkh} e_{kh}^y \Big(\boldsymbol{U}^{rs}(\boldsymbol{y}) \Big) \Big\rangle \tag{2.6}$$

It can easily be shown that

$$\frac{1}{|Y|} \int_{\partial Y} \frac{1}{2} (U_k^{rs} n_h + U_h^{rs} n_k) \, dS = \delta_{sk} \delta_{rh} \tag{2.7}$$

3. Effective moduli for a network of elastic rods

For a periodical network of elastic rods the effective moduli q_{ijrs} are written in the form

$$q_{ijrs} = \frac{1}{|Y|} \int_{Y_t} \Pi_{ij}^{rs} \, dy \qquad \Pi_{ij}^{rs} = a_{ijkh} e_{kh} \Big(\boldsymbol{U}^{rs}(\boldsymbol{y}) \Big) \tag{3.1}$$

The local problem (2.4) is now rewritten as follows

$$\begin{aligned} & -\frac{\partial}{\partial y} a_{xijkh} \Big(e_{kh}^y \Big(\boldsymbol{U}^{rs}(\boldsymbol{y}) \Big) = 0 \quad \text{in } Y_t \\ & e_{kh}^y \Big(\boldsymbol{U}^{rs}(\boldsymbol{y}) \Big) \Big|_{\partial Y_+} = e_{kh}^y \Big(\boldsymbol{U}^{rs}(\boldsymbol{y}) \Big) \Big|_{\partial Y_-} \\ & \Pi_{ij}^{rs} N_j = 0 \quad \text{on } \partial Y_t' \qquad \partial Y_t = \partial Y_t' \cap \partial Y_+ \cap \partial Y_- \end{aligned} \tag{3.2}$$

Here Y_t, ∂Y_t, ∂Y_+, ∂Y_- denote the region occupied by the elastic rods, the boundary of the region of elastic rods, and the opposite walls of the basic cell, respectively.

3.1. Formula for the effective modulus

To solve the basic cell problem we proceed in a manner typical of structual mechanics. Let us introduce the Cartesian coordinate system $\boldsymbol{y}^{PZ}(y_1^{PZ}, y_2^{PZ}, y_3^{PZ})$, $P = A, B, C, D, ...$, $Z = A, B, C, D, ...$, $P \neq Z$, coincident with the principal inertia axes of a (PZ)th rod of a length l^{PZ}. Note that the y_3^{PZ} axis always runs along the longest dimension of a (PZ)th rod (Fig.5). Consider also a Cartesian coordinate system $\{y_i\}$, $i = 1, 2, 3$, firmly connected with the basic cell. The orientation of $\{y_i^{PZ}\}$ with respect to $\{y_i\}$, $i = 1, 2, 3$, is determined by the directional cosines L_{ij}^{PZ}. For the sake of simplicity the intersection points $(A, B, G, H, ...)$ of the axes of the elastic rods we call the *network nodes*.

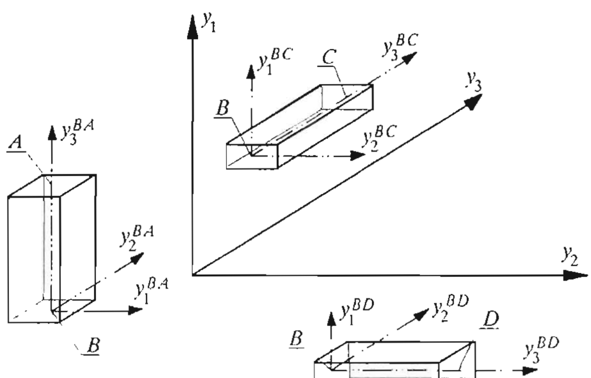

Fig. 5. Cartesian coordinates $Y^{PZ}(y_1^{PZ}, y_2^{PZ}, y_3^{PZ})$ and $Y(y_1, y_2, y_3)$ connected with the elastic rod

We assume that the domains of rod junctions of the network are much smaller than the volumes of individual rods. Hence, from Eq (3.4) it follows that the averaged stresses $\left[\Pi_{ij}^{rs}\right]^{PZ}$ defined by

$$\left[\Pi_{ij}^{rs}\right]^{PZ} = \frac{1}{S^{PZ}} \int\limits_{S^{PZ}} \Pi_{ij}^{rs}\, dS^{PZ} \tag{3.3}$$

do not depend on y_3^{PZ}, where S^{PZ} denote the cross-section of a (PZ)th rod. Hence the definition (3.1) reduces to

$$q_{ijrs} = \frac{1}{|Y|} \sum_{PZ} L_{ik}^{PZ} L_{jm}^{PZ} \left[\Pi_{km}^{rs}\right]^{PZ} |Y|^{PZ} \tag{3.4}$$

Here $|Y|^{PZ}$ denotes the volume of (PZ)th rod. For a particular (PZ)th elastic rod it is convenient to introduce the following notation

$$
\begin{aligned}
&(T_h^{rs})^{PZ} = S^{PZ}\Big[\Pi_{ij}^{rs}\Big]^{PZ} n_3 = \int\limits_{S^{PZ}} (\Pi_{h3}^{rs})^{PZ} n_3 \; dS \qquad h = 1,2,3\\
&(M_1^{rs})^{PZ} = \int\limits_{S^{PZ}} y_2 (\Pi_{33}^{rs})^{PZ} n_3 \; dS \qquad (M_2^{rs})^{PZ} = \int\limits_{S^{PZ}} y_1 \Pi_{33}^{rs} n_3 \; dS\\
&(M_3^{rs})^{PZ} = \int\limits_{S^{PZ}} y_2^{PZ} (\Pi_{13}^{rs})^{PZ} n_3 - y_1^{PZ} (\Pi_{23}^{rs})^{PZ} n_3 \; dS \qquad (3.5)\\
&(\omega_1^{rs})^{SZ} = \frac{\partial (w_2^{rs})^{SZ}}{\partial y_3^{SZ}} \qquad (\omega_2^{rs})^{SZ} = \frac{\partial (w_1^{rs})^{SZ}}{\partial y_3^{SZ}}\\
&(\omega_3^{rs})^{SZ} = \varphi \qquad (w_k^{rs})^{PZ}(y_3^{PZ}) = (U_k^{rs})^{PZ}(0,0,y_3^{PZ})
\end{aligned}
$$

where φ – rotation angel and the vector functions

$$
\begin{aligned}
&(\boldsymbol{T}^{rs})^{PZ}(T_1^{rs}, T_2^{rs}, T_3^{rs}) \qquad (\boldsymbol{M}^{rs})^{PZ}(M_1^{rs}, M_2^{rs}, M_3^{rs})\\
&(\boldsymbol{w}^{rs})^{PZ}(w_1^{rs}, w_2^{rs}, w_3^{rs}) \qquad (\boldsymbol{\omega}^{rs})^{PZ}(\omega_1^{rs}, \omega_2^{rs}, \omega_3^{rs})
\end{aligned}
\qquad (3.6)
$$

represent shear and normal forces, moments, nodal displacements only and rotations angles associated with the cross-section normal to the longest axis of the (PZ)th rod (Fig.5).

3.2. The basic cell problem for network of rods

For a network of elastic rods the basic cell problem (3.2) reduces to the following algebraic relations given bellow.

3.2.1. Equations for an individual elastic rod

From Eqs $(3.2)_1$ and (3.5) one easily obtains the formulae for:
(i) The difference between the displacements of the points P and Z (see Fig.6)

$$
\begin{aligned}
w_1^{rs}(Z) - w_1^{rs}(P) &= \frac{1}{EJ_1}\Big(\frac{1}{2}M_2^{rs}(P)l^2 + \frac{1}{6}T_1^{rs}(P)l^3 + \omega_2^{rs}(P)l\Big)\\
w_2^{rs}(Z) - w_2^{rs}(P) &= \frac{1}{EJ_2}\Big(\frac{1}{2}M_1^{rs}(P)l^2 + \frac{1}{6}T_2^{rs}(P)l^3 + \omega_1^{rs}(P)l\Big) \qquad (3.7)\\
w_3^{rs}(Z) - w_3^{rs}(P) &= -\frac{T_3^{rs}(P)l}{ES}
\end{aligned}
$$

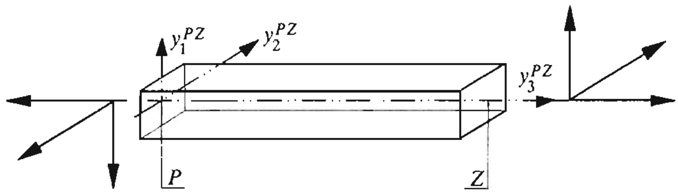

Fig. 6. External vectors represent: the displacements $\boldsymbol{w}^{PZ}(w_1^{PZ}(P), w_2^{PZ}(P), w_3^{PZ}(P))$, $\boldsymbol{w}^{PZ}(w_1^{PZ}(Z), w_2^{PZ}(Z), w_3^{PZ}(Z))$; the rotation angles $\boldsymbol{\omega}^{PZ}(\omega_1^{PZ}(P), \omega_2^{PZ}(P), \omega_3^{PZ}(P))$, $\boldsymbol{\omega}^{PZ}(\omega_1^{PZ}(Z), \omega_2^{PZ}(Z), \omega_3^{PZ}(Z))$; the shear forces $\boldsymbol{T}^{PZ}(T_1^{PZ}(P), T_2^{PZ}(P), T_3^{PZ}(P))$, $\boldsymbol{T}^{PZ}(T_1^{PZ}(Z), T_2^{PZ}(Z), T_3^{PZ}(Z))$ and moments $\boldsymbol{M}^{PZ}(M_1^{PZ}(P), M_2^{PZ}(P), M_3^{PZ}(P))$, $\boldsymbol{M}^{PZ}(M_1^{PZ}(Z), M_2^{PZ}(Z), M_3^{PZ}(Z))$ acting at the ends of the elastic PZth rod

(ii) The difference between the rotation angles of the axis ends of the (PZ)th rod

$$
\begin{aligned}
\omega_1^{rs}(Z) - \omega_1^{rs}(P) &= \frac{1}{EJ_2}\Big(M_1^{rs}(P)l + \frac{1}{2}T_2^{rs}(P)l^2\Big) \\
\omega_2^{rs}(Z) - \omega_2^{rs}(P) &= \frac{1}{EJ_1}\Big(M_2^{rs}(P)l + \frac{1}{2}T_1^{rs}(P)l^2\Big) \\
\omega_3^{rs}(Z) - \omega_3^{rs}(P) &= -\frac{M_3^{re}(P)l}{D}
\end{aligned}
\tag{3.8}
$$

(iii) The equilibrium equations for the forces and moments acting on the (PZ)th rod

$$
\begin{aligned}
T_2^{rs}(Z) + T_2^{rs}(P) &= 0 \qquad & M_1^{re}(P) + T_2^{rs}(P)l + M_1^{rs}(Z) &= 0 \\
T_1^{rs}(Z) + T_1^{rs}(P) &= 0 \qquad & M_2^{re}(P) + T_1^{rs}(P)l + M_2^{rs}(Z) &= 0
\end{aligned}
\tag{3.9}
$$

3.2.2. Static and kinematic conditions for nodes

For an arbitrary node point $P = A, B, C$, of the network the following relations are valid:

(i) The equilibrium equations for forces and moments acting on the (P)th node

$$
\begin{aligned}
&\sum_Z (T_m^{rs})^{PZ}(P)L_{km}^{PZ} = 0 \qquad Z = A, B, \ldots \neq P \quad k, m = 1, 2, 3 \\
&\sum_Z (M_m^{rs})^{PZ}(P)L_{km}^{PZ} = 0 \qquad Z = A, B, \ldots \neq P \quad k, m = 1, 2, 3
\end{aligned}
\tag{3.10}
$$

(ii) The displacement compatibility equations for the (P)th node

$$(w_m^{rs})^{PZ}(P)L_{km}^{PZ} = (w_m^{rs})^{PQ}(P)L_{km}^{PQ} \qquad Q = A, B, C, ... \tag{3.11}$$

(iii) The rotation compatibility equations for the (P)th node

$$(\omega_m^{rs})^{PZ}(P)L_{km}^{PZ} = (\omega_m^{rs})^{PQ}(P)L_{km}^{PQ} \qquad Q = A, B, C, ... \tag{3.12}$$

3.2.3. Boundary conditions prescribed on the basic cell faces

On the basic cell faces the following boundary conditions have to be prescribed

$$\begin{gathered} e_{kh}\Big(\boldsymbol{w}^{rs}(\boldsymbol{y})\Big)\Big|_{\partial Y_+} = e_{kh}\Big(\boldsymbol{w}^{rs}(\boldsymbol{y})\Big)\Big|_{\partial Y_-} \\ \frac{1}{|Y|}\sum_{n=1}^{N}\frac{1}{2}(w_k^{rs}n_h + w_h^{rs}n_k)\partial Y_n = \delta_{sk}\delta_{rh} \quad \text{on } \partial Y = \partial Y_1 \cup \partial Y_2 \cup ... \cup \partial Y_N \end{gathered} \tag{3.13}$$

Eqs (3.4) $\div$ (3.13) allow us to evaluate the homogenized moduli for an arbitrary network of thin elastic rods with a periodic structure.

4. Illustrative example

As an example we evaluate the effective elastic moduli for a regular network of elastic rods shown in Fig.7. This network represents the microstructure of cancellous bone (see Fig.2 and Fig.3).

It is convenient to split the considered basic cell into two parts shown in Fig.8.

Next we proceed as in Fig.9, Without loss of generality we can consider only the fragment of the network depicted in Fig. 9b.

4.1. The effective coefficients q_{ijkl}

Now we can evaluate the effective coefficients q_{ijkl} for the network of elastic rods characterized by the unit cell shown in Fig.7. To this end we apply the homogenization procedure proposed in Section 3. First we decompose the fragment b of the basic cell (Fig.9b) into four individual rods, see Fig.10. Only the displacements due to bending are taken into account.

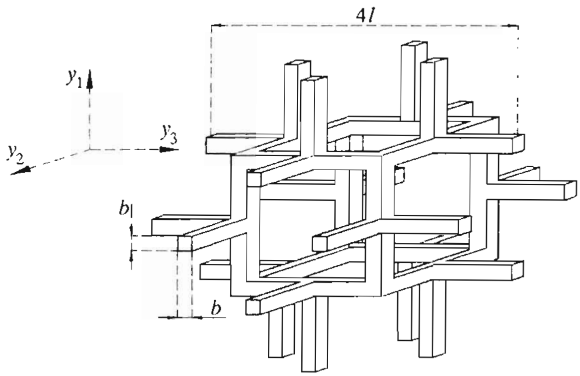

Fig. 7. Basic cell for a network of elasic rods modelling the microstructure of a cancellous bone depicted in Fig.2 and Fig.3

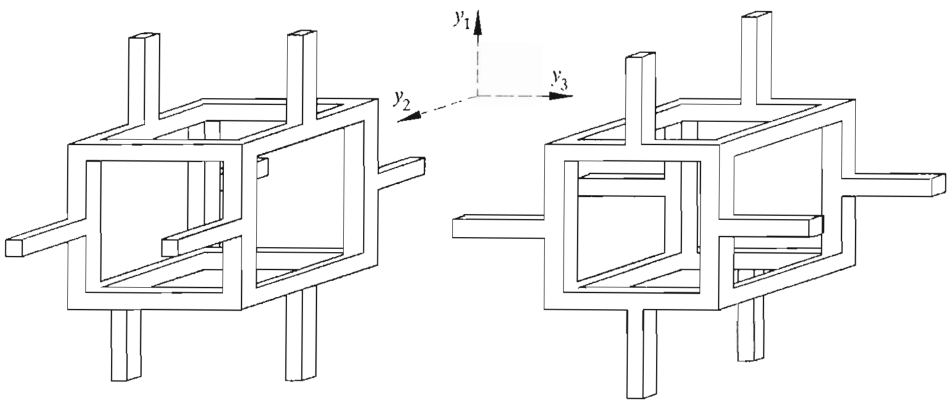

Fig. 8. Two rod like microstructures generated by the basic cell shown in Fig.7

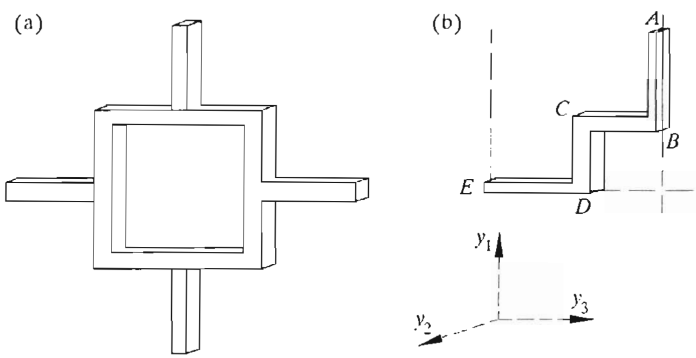

Fig. 9. Further decomposition of the basic cell

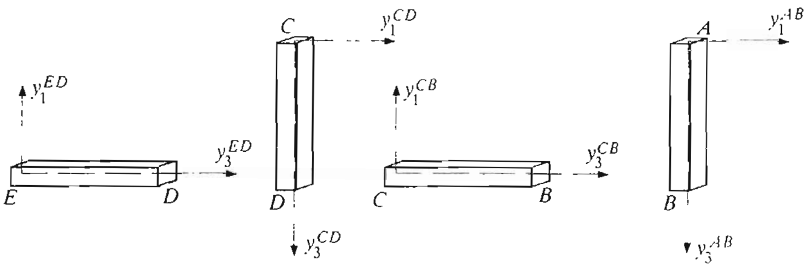

Fig. 10. Individul elastic rods forming the structure shown in Fig.9

4.1.1. The coefficients q_{1212}, q_{2323}, q_{1313}

On account of the symmetry of the structure (Fig.7) we obtain

$$q_{1212} = q_{2323} = q_{1313} \tag{4.1}$$

Hence, only the coefficient q_{1212} will be evaluated. For an individual (PZ)th rod Eqs (3.7) $\div$ (3.9) take the form, see Fig.10

$$\begin{aligned}
&w_1^{AB}(A) - w_1^{AB}(B) = \frac{1}{EJ}\Big(\frac{1}{2}M_2^{AB}(B)l^2 + \frac{1}{6}T_1^{AB}(B)l^3 + \omega_2^{AB}(B)l\Big)\\
&w_1^{ED}(E) - w_1^{ED}(D) = \frac{1}{EJ}\Big(\frac{1}{2}M_2^{ED}(D)l^2 + \frac{1}{6}T_1^{ED}(D)l^3 + \omega_2^{ED}(D)l\Big)\\
&M_2^{AB}(B) + T_1^{AB}(B)l + M_2^{AB}(A) = 0 \qquad\qquad T_1^{AB}(A) + T_1^{AB}(B) = 0\\
&M_2^{ED}(D) + T_1^{ED}(D)l + M_2^{ED}(E) = 0 \qquad\qquad T_1^{ED}(E) + T_1^{ED}(D) = 0
\end{aligned} \tag{4.2}$$

The boundary conditions are implied by Eq (2.7) and are given by

$$\begin{aligned}
&w_1^{AB}(A) = -2l \qquad M_2^{AB}(A) = 0 \qquad \omega_2^{AB}(B) = 0\\
&w_1^{ED}(E) = 2l \qquad M_2^{ED}(E) = 0 \qquad \omega_2^{ED}(D) = 0
\end{aligned} \tag{4.3}$$

By solving Eqs (4.2) and (4.3) we arrive at

$$T_1^{AB} = \frac{6EJ}{l^2} \qquad\qquad T_1^{ED} = \frac{6EJ}{l^2} \tag{4.4}$$

Hence, by virtue of Eq (3.4) one obtains immediately

$$q_{1212} = q_{2323} = q_{1313} = \frac{4lT_1^{AB}}{32l^3} = \frac{3EJ}{4l^4} \tag{4.5}$$

4.1.2. The coefficients q_{1111}, q_{2222}, q_{3333}, q_{1122}, q_{2233}, q_{1133}

Now we pass to evaluation of the elastic moduli q_{1111}, q_{2222}, q_{3333}, q_{1122}, q_{2233}, q_{1133}. Let us first estimate the coefficient q_{1111}. For the points D and B, in Fig.9 and Fig.10, the boundary conditions are as follows (see Eq (2.7))

$$\begin{aligned} &w_1^{CB}(B) = -2l \qquad && \omega_2^{AB}(B) = 0 \\ &w_1^{CD}(D) = 0 && \omega_2^{CD}(D) = 0 \end{aligned} \tag{4.6}$$

The relative displacements of the points A and B and C and D are given by

$$\begin{aligned} w_1^{CB}(B) - w_1^{CB}(C) &= \frac{1}{EJ}\Big(\frac{1}{2}M_2^{CB}(C)l^2 + \frac{1}{6}T_1^{CB}(C)l^3 + \omega_2^{CB}(C)l\Big) \\ w_1^{CD}(D) - w_1^{CD}(C) &= \frac{1}{EJ}\Big(\frac{1}{2}M_2^{CD}(C)l^2 + \frac{1}{6}T_1^{CD}(C)l^3 + \omega_2^{CD}(C)l\Big) \end{aligned} \tag{4.7}$$

The relations

$$\begin{aligned} \omega_2^{CB}(B) - \omega_2^{CB}(C) &= \frac{1}{EJ}\Big(M_2^{CB}(C)l + \frac{1}{2}T_1^{CB}(C)l^2\Big) \\ \omega_2^{CD}(D) - \omega_2^{CD}(C) &= \frac{1}{EJ}\Big(M_2^{CD}(C)l + \frac{1}{2}T_1^{CD}(C)l^2\Big) \end{aligned} \tag{4.8}$$

determine the relative rotations of the axis ends of the rods AB and CD. The forces acting at points A, B, C, D satisfy

$$\begin{aligned} &M_2^{CB}(C) + T_1^{CB}(C)l + M_2^{CB}(B) = 0 \qquad && T_1^{CB}(C) + T_1^{CB}(B) = 0 \\ &M_2^{CD}(C) + T_1^{CD}(C)l + M_2^{CD}(B) = 0 && T_1^{CD}(C) + T_1^{CD}(D) = 0 \end{aligned} \tag{4.9}$$

For a node C we have

$$\begin{aligned} &M_2^{CB}(C) + M_2^{CD}(C) = 0 \qquad && \omega_2^{CB}(C) = \omega_2^{CD}(C) \\ &w_1^{CB}(C) = 0 && w_1^{CD}(C) = 0 \end{aligned} \tag{4.10}$$

We obtain 16 equations with 16 unknown functions. By using Eqs (4.10) the relations (4.7) and (4.8) yield

$$\begin{aligned} 2l &= \frac{1}{EJ}\Big(\frac{1}{2}M_2^{CB}(C)l^2 + \frac{1}{6}T_1^{CB}(C)l^3 + \omega_2^{CB}(C)l\Big) \\ 0 &= \frac{1}{EJ}\Big(\frac{1}{2}M_2^{CD}(C)l^2 + \frac{1}{6}T_1^{CD}(C)l^3 + \omega_2^{CD}(C)l\Big) \end{aligned} \tag{4.11}$$

Then the rotation angles are given by

$$\begin{aligned} -\omega_2^{CB}(C) &= \Big(M_2^{CB}(C)l + \frac{1}{2}T_1^{CB}(C)l^2\Big) \\ -\omega_2^{CB}(C) &= \Big(-M_2^{CB}(C)l + \frac{1}{2}T_1^{CD}(C)l^2\Big) \end{aligned} \tag{4.12}$$

By adding and substracting the right and left hand sides of the last two equations we obtain

$$\begin{aligned} \omega_2^{CB}(C) &= -\frac{1}{4}T_1^{CD}(C)l^2 - \frac{1}{4}T_1^{CB}(C)l^2 \\ M_2^{CB}(C)l &= -\frac{1}{4}T_1^{CB}(C)l^2 + \frac{1}{4}T_1^{CD}(C)l^2 \end{aligned} \tag{4.13}$$

From Eqs (4.11) and (4.13) we conclude that

$$\begin{aligned} 2l &= \frac{1}{EJ}\Big(\frac{5}{24}T_1^{CB}(C)l^3 + \frac{1}{8}T_1^{CD}(C)l^3\Big) \\ 0 &= \frac{1}{EJ}\Big(\frac{1}{8}T_1^{CB}(C)l^3 + \frac{5}{24}T_1^{CD}(C)l^3\Big) \end{aligned} \tag{4.14}$$

Consequently

$$T_1^{CD}(C) = -\frac{9EJ}{l^2} \qquad\qquad T_1^{CB}(C) = \frac{15EJ}{l^2} \tag{4.15}$$

Thus the normal forces acting on the rods AB, BC, CD and DE are

$$\begin{aligned} T_3^{AB}(C) &= \frac{15EJ}{l^2} \qquad\qquad & T_3^{CD}(C) &= \frac{15EJ}{l^2} \\ T_3^{ED}(C) &= \frac{9EJ}{l^2} \qquad\qquad & T_3^{CB}(C) &= \frac{9EJ}{l^2} \end{aligned} \tag{4.16}$$

Finally, we find

$$\begin{aligned} q_{1111} &= \frac{8T_3^{AB}(C) + 8T_3^{CD}(C)}{32l^3} = \frac{15EJ}{2l^4} \\ q_{1122} &= \frac{2T_3^{ED}(C) + 2T_3^{CB}(C)}{32l^3} = \frac{9EJ}{4l^4} \end{aligned} \tag{4.17}$$

and

$$q_{1111} = q_{2222} = q_{3333} \qquad\qquad q_{1122} = q_{1133} = q_{3322} \tag{4.18}$$

4.1.3. *The coefficients C_{ij} and $(C_{ij})^{-1}$*

Now we are in position to present the effective moduli in a matrix form. Accordingly, we replace the tensors q_{klmn} and $(q_{klmn})^{-1}$ by C_{ij} and $(C_{ij})^{-1}$ (cf Nowacki, 1970). We also set $E = E_s$, where E_s denotes the Young modulus of the cancellous bone rod. Taking into account Eqs (4.5) and (4.8) and setting $\mathbf{A} = \mathbf{C}^{-1}$ we write

$$\mathbf{C} = \begin{bmatrix} \frac{15E_sJ}{2l^4} & \frac{9E_sJ}{4l^4} & \frac{9E_sJ}{4l^4} & 0 & 0 & 0 \\ \frac{9E_sJ}{4l^4} & \frac{15E_sJ}{2l^4} & \frac{9E_sJ}{4l^4} & 0 & 0 & 0 \\ \frac{9E_sJ}{4l^4} & \frac{9E_sJ}{4l^4} & \frac{15E_sJ}{2l^4} & 0 & 0 & 0 \\ 0 & 0 & 0 & \frac{3E_sJ}{4l^4} & 0 & 0 \\ 0 & 0 & 0 & 0 & \frac{3E_sJ}{4l^4} & 0 \\ 0 & 0 & 0 & 0 & 0 & \frac{3E_sJ}{4l^4} \end{bmatrix} \tag{4.19}$$

$$\mathbf{A} = \begin{bmatrix} \frac{13l^4}{84E_sJ} & -\frac{l^4}{28E_sJ}l^4 & -\frac{l^4}{28E_sJ} & 0 & 0 & 0 \\ -\frac{l^4}{28E_sJ} & \frac{13l^4}{84E_sJ} & -\frac{l^4}{28E_sJ} & 0 & 0 & 0 \\ -\frac{l^4}{28E_sJ} & -\frac{l^4}{28E_sJ} & \frac{13l^4}{84E_sJ} & 0 & 0 & 0 \\ 0 & 0 & 0 & \frac{4l^4}{3E_sJ} & 0 & 0 \\ 0 & 0 & 0 & 0 & \frac{4l^4}{3E_sJ} & 0 \\ 0 & 0 & 0 & 0 & 0 & \frac{4l^4}{3E_sJ} \end{bmatrix}$$

For the investigated microstructure the technical effective coefficients are

$$E^* = \frac{1}{A_{11}} = \frac{84E_sJ}{13l^4} \qquad \nu^* = -\frac{A_{12}}{A_{11}} = 0.23 \qquad G^* = \frac{1}{A_{44}} = \frac{3E_sJ}{4l^4} \tag{4.20}$$

Here E^*, ν^*, G^* denote the overall Young modulus, Poisson ratio and shear modulus, respectively.

4.1.4. Rods with asquare cross-section

As a numerical example we evaluate the theoretical moduli C_{11}, C_{12}, C_{44} and technical coefficients E^*, ν^*, G^* in the case of square cross-sections of elastic rods.

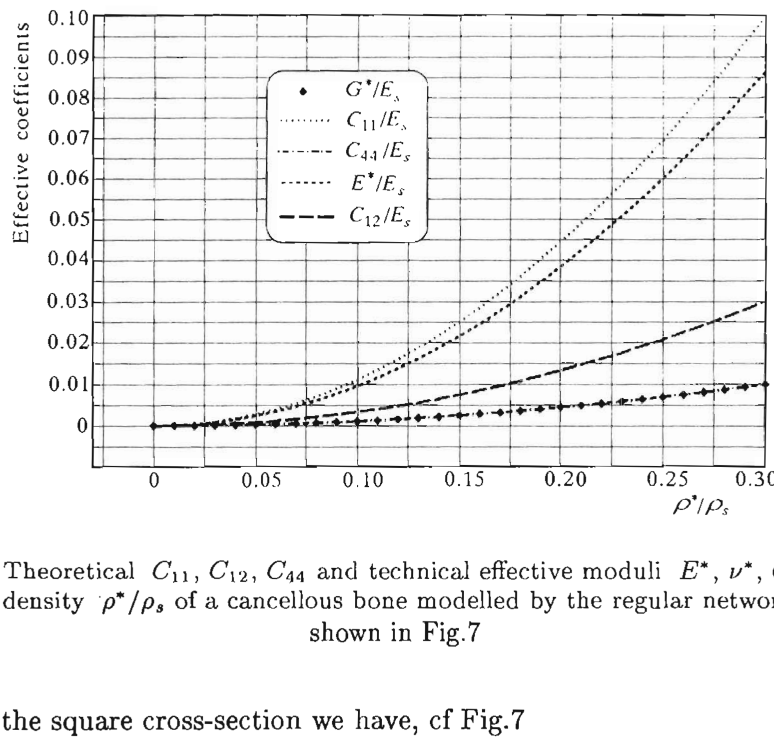

Fig. 11. Theoretical C_{11}, C_{12}, C_{44} and technical effective moduli E^*, ν^*, G^* versus relative density ρ^*/ρ_s of a cancellous bone modelled by the regular network of rods shown in Fig.7

For the square cross-section we have, cf Fig.7

$$J = \frac{1}{12}b^4 \qquad \frac{\rho^*}{\rho_s} = \frac{\frac{m_c}{64l^3}}{\frac{m_c}{48lb^2}} = \frac{3}{4}\frac{b^2}{l^2} \tag{4.21}$$

Here ρ^*, ρ_s and m^* denote: apparent density of the cancellous bone, density of the solid bone forming the cancellous bone and mass of the basic cell.

By virtue of Eqs (4.5), (4.17) and (4.21) we get

$$C_{44} = C_{55} = C_{66} = 0.11\Big(\frac{\rho^*}{\rho_s}\Big)^2 \qquad C_{11} = C_{22} = C_{33} = 1.11E_s\Big(\frac{\rho^*}{\rho_s}\Big)^2$$

$$C_{12} = C_{12} = C_{12} = 0.34E_s\Big(\frac{\rho^*}{\rho_s}\Big)^2 \tag{4.22}$$

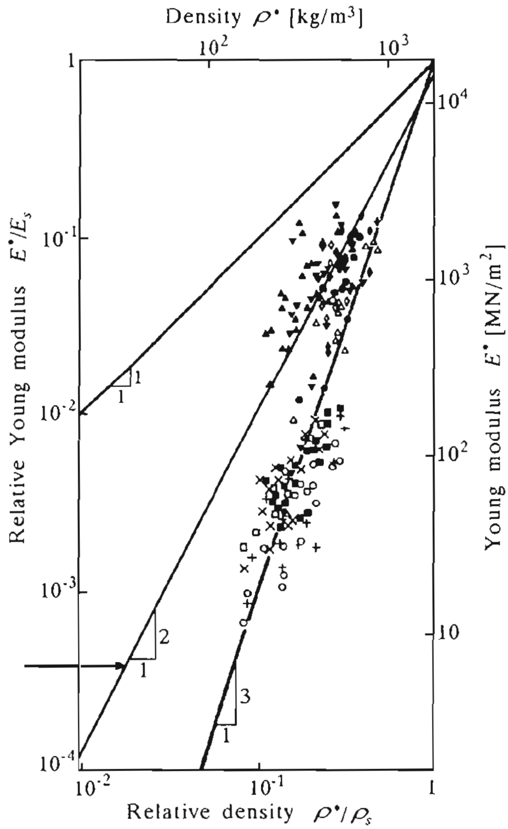

Fig. 12. Young moduli of cancellous bone of unspecified trabecular orientation plotted against density. Normalizing parameters are: $E_s = 17\,\mathrm{GN/m^2}$ and $\rho_s = 1800\,\mathrm{kg/m^3}$. The experimental data from Gibson and Ashby (1988). The line with the slope 2 (pointed out by the arrow) was obtained in this paper. The lines with slope 1 and 2 are drawn for comparison

Finally, we arive at

$$\frac{C}{\left(\frac{\rho^*}{\rho_s}\right)^2 E_s} = \begin{bmatrix} 1.11 & 0.34 & 0.34 & 0 & 0 & 0 \\ 0.34 & 1.11 & 0.34 & 0 & 0 & 0 \\ 0.34 & 0.34 & 1.11 & 0 & 0 & 0 \\ 0 & 0 & 0 & 0.11 & 0 & 0 \\ 0 & 0 & 0 & 0 & 0.11 & 0 \\ 0 & 0 & 0 & 0 & 0 & 0.11 \end{bmatrix} \tag{4.23}$$

From Eqs (4.20) and (4.10) we get

$$\frac{E^*}{E_s} = 0.96\Big(\frac{\rho^*}{\rho_s}\Big)^2 \qquad \frac{G^*}{E_s} = 0.11\Big(\frac{\rho^*}{\rho_s}\Big)^2 \qquad v^* = 0.23 \tag{4.24}$$

The moduli C_{11}/E_s, C_{12}/E_s, C_{44}/E_s, G^*/E_s and E^*/E_s versus ρ^*/ρ_s are depicted in Fig.11. The comparison of E^*/E_s with experimental data is presented in Fig.12.

5. Concluding remarks

The macroscopic cancellous bone is characterized by three independent material constants, being therefore, a material with cubic symmetry (cf Chernykh, 1988). A cancellous bone is rather an orthotropic material (Jemioło and Telega, 1998). The orthotropic macroscopic model can easily be incorporated into our modelling by taking basic cells with different sizes along the axes y_i, $i = 1,2,3$. Though the normal forces and torsion were neglected, our approach leads to the results which compare favourably with the available experimental ones.

Acknowlegment

The work was suported by the State Committe for Scientific Research (KBN, Poland) under grants No. 8 T11F 018 12 and 7 T07A 021 15.

References

1. BEAUPRÉ G.S., HAYES W.C., 1985, Finite Element Analysis of a Three Dimensional Opened-Celled Model for Trabecular Bone, *J. Biomech. Engng.*, **107**, 249-256
2. BENDSØE M.P., 1995, *Optimization of Structural Topology, Shape, and Material*, Springer-Verlag, Berlin
3. BENDSØE M.P., KIKUCHI N., 1988, Generating Optimal Topologies in Structural Design Using a Homogenization Method, *Comp. Mech. Appl. Mech. Enging.*, **71**, 192-224
4. BENSOUSSAN A., LIONS J.L., PAPANICOULAOU G., 1978, *Asymptotic Analysis for Periodic Structures*, North-Holland, Amsterdam
5. CHERNYKH K.F., 1988, *Introduction to Anisotropic Elasticity*, Nauka, Moskwa, in Russian
6. COWIN S.C., 1989a, The Mechanical Properties of Cortical Bone Tissue, in: *Bone Mechanics*, edit. by S.C. Cowin, 97-127, CRC Press, Inc. Boca Raton, Florida

7. COWIN S.C., 1989b, The Mechanical Properties of Cancellous Bone, in: *Bone Mechanics*, edit. by S.C. Cowin, 129-157, CRC Press, Inc. Boca Raton, Florida

8. CROLET J.M., 1990, Homogenization: Mathematical Method Applied to Haversian Cortical Bone Structure, *Proc. 1st World Congress of Biomechanics*, 156-172

9. CROLET J.M., AOUBIZA B., MEUNIER A., 1993, Compact Bone: Numerical Simulation of Mechanical Characteristics, *J. Biomechanics*, **26**, 677-687

10. DAL MASO G., 1993, *Introdution to* Γ*-Convergence*, Birkhäuser, Boston

11. GAŁKA A., TELEGA J.J., TOKARZEWSKI S., 1999, Application of Homogenization to Evaluation of Effective Moduli of Linear Elastic Trabecular Bone with Plate – Like Structure, *Arch. Mech.*, **51**, 3

12. GIBSON J.L., 1985, The Mechanical Behaviour of Cancellous Bone, *J. Biomechanics*, **18**, 317-328

13. GIBSON J.L., ASHBY M.F., 1988, *Cellular Solids: Structure and Properties*, Pergamon Press, New York

14. HOLLISTER S.J., BRENNAN J.M., KIKUCHI N., 1994, A Homogenization Sampling Procedure for Calculating Trabecular Bone Effective Stiffness and Tissue Level Stress, *J. Biomechanics*, **27**, 433-444

15. HOLLISTER S.J., FYHIRE D.P., JEPSEN K.J., GOLDSTEIN S.A., 1991, Application of Homogenization Theory to the Study of Trabecular Bone Mechanics, *J. Biomechanics*, **24**, 825-839

16. JEMIOŁO S., TELEGA J.J., 1998, Fabric Tensors in Bone Mechanics, *Engng. Trans.*, **46**, 3-26

17. JIKOV V.V., KOZLOV S.M., OLEINIK O.A., 1994, *Homogenization of Differential Operators and Integral Functionals*, Springer-Verlag, Berlin

18. KASRA M., GRYNPAS M.D., 1998, Static and Dynamic Finite Element Analyses of an Idealized Structural Model of Vertebral Trabecular Bone, *J. Biomech. Eng.*, **120**, 267-272

19. KATZ J.L., 1976, Hierarchical Modelling of Compact Bone as a Fiber Reinforced Material, in: *Advances in Bioengineering*, edit. by R.E. Mates and C.R Smith, 18-19, American Society of Mechanical Engineers, New York

20. KOHN R.V., STRANG G., 1986, Optimal Design and Relaxation of Variational Problems, I, II, III, *Comm. Pure Appl. Math.*, **39**, 113-137, 139-182, 353-377

21. LEWIŃSKI T., TELEGA J.J., 1999, *Plates, Laminates and Shells: Asymptotic Analysis and Homogenization*, World Scientific, in press

22. LOWET G., RÜEGSEGGER P., WEINANS H., MEUNIER A. (edit.), 1997, *Bone Research in Biomechanics*, IOS Press, Amsterdam

23. LURIE K.A., FEDOROV A.V., CHERKAEV A.V., 1982, Regularization of Optimal Design Problems for Bars and Plates, I and II, *J. Opt. Theory Appl.*, **37**, 499-522, 523-543

24. MCELHANEY J., ALEM N., ROBERTS V., 1970, A Porous Block Model for Cancellous Bones, *ASME Publication* No. 70-WA//BHF-2, 1-9

25. MÜLLER R., RÜEGSEGGER P., 1997, Micro-Tomographic Imaging for the Nondestructive Evaluation of Trabecular Bone Architecture, in: *Bone Research in Biomechanics*, edit. by G. Lowet, P. Rüegsegger, H. Weinans and A. Meunier, 61-79, IOS Press, Amsterdam

26. NOWACKI W., 1970, *Elasticity Theory*, Państwowe Wydawnictwo Naukowe, Warszawa, in Polish

27. PAYTEN W.M., BEN-NISSAN B., MERCER D.J., 1998, Optimal Topology Design Using Global Self-Organisational Approach, *Int. J. Solids Structures*, **35**, 219-237

28. PUGH J.W., ROSE R.M., RADIN E.L., 1973, A Structural Model for the Mechanical Behavior of Trabecular Bone, *J. Biomechanics*, **6**, 657-670

29. SANCHEZ-PALENCIA E., 1980, *Non-Homogeneous Media and Vibration Theory*, Springer-Verlag, Berlin

30. SMITH J. W., 1960, The Arrangement of Collagen Fibers in Human Secondary Osteons, *J. Bone Joint Surgery*, **42B**, 588

31. TELEGA J.J., GAŁKA A., TOKARZEWSKI S., 1999, Application of Reiterated Homogenization to Determination of Effective Moduli of Compact Bone, *J. Theor. Appl. Mech.*, **37**, 3

32. TOKARZEWSKI S., GAŁKA A., TELEGA J.J., 1998, Cancellous Bone as a Cellular Solid: the Determination of Effective Material Properties, in: *Proc. of the Conf. on Biomechanics: Modelling, Computational Methods, Experiments and Biomedical Applications*, edit. by J. Awrejcewicz, M. Ciach and M. Kleiber, 191-196, Technical University of Łódź, in Polish

33. ULRICH D., HILDEBRAND T., VAN RIETBERGEN B., MÜLLER R., RÜEGSEGGER P., 1997, The Quality of Trabecular Bone Evaluated with Micro-Computed Tomography, FEA and Mechanical Testing, in: *Bone Research in Biomechanics*, edit. by G. Lovet, P. Rüegsegger, H. Weinans and A. Meunier, 97-112, IOS Press, Amsterdam

34. WARREN W.E., KRAYNIK A.M., 1997, Linear Elastic Behavior of Low-Density Kelvin foam with Open Cells, *J.Appl. Mech.*, **64**, 787-794

35. WILLIAMS J.L., LEWIS J.L., 1982, Properties and Anisotropic Model of Cancellous Bone from the Proximal Tibia Epiphysis, *J. Biomech. Engng.*, **104**, 50-56

36. ZYSSET P.K., GOULET R.W., HOLLISTER S.J., 1998, A Global Relationship Between Trabecular Bone Morfology and Homogenized Elasic Properties, *J. Biomech. Eng.*, **120**, 640-646

Wyznaczanie efektywnych modułów sprężystych dla kości gąbczastej o regularnej strukturze beleczkowej

Streszczenie

Teorię homogenizacji zastosowano do wyznaczania efektywnych własności mechanicznych dla regularnej sieci elastycznych prętów modelujących kość gąbczastą. Wyznaczono numerycznie efektywne stałe techniczne: moduł Younga, współczynnik Poissona i moduł ścinania. Wyniki porównano z wynikami eksperymentalnymi uzyskując dobrą zgodność.

Manuscript received February 4, 1999; accepted for print March 3, 1999